Computational Paradigms using Oscillatory Networks based on State-Transition Devices

Abhinav Parihar*, Nikhil Shukla†, Matthew Jerry†, Suman Datta†, Arijit Raychowdhury*
* School of Electrical and Computer Engineering,
Georgia Institute of Technology,
Atlanta, GA - 30332
† Department of Electrical Engineering,
University of Norte Dame,
Notre Dame, IN - 46556

***Abstract*—In this paper we review recent work on computational paradigms involving coupled relaxation oscillators built using metal-insulator-transition (MIT) devices. Such oscillators made using MIT devices based on Vanadium-Dioxide thin films are very compact and can be realized in hardware. Networks of such oscillators have interesting phase and frequency dynamics which can be programmed to solve computationally hard problems.**

I. Introduction

Building systems using a physical substrate that can compute involves (a) understanding what is needed for computing, and (b) what computing properties are offered by the substrate. It is this complimenting match that makes a system computationally powerful and efficient. From the dawn of research in computing, the digital symbolic metaphor has been prevalent wherein information is represented symbolically as binary bits and these bits are transformed for any operation on these quantities. As such, most of research efforts have been focussed on creating better "switches", i.e. representing and modifying binary information or bits using physical substrates, or electronic devices. The possibility that physical devices can offer more computing abilities than just a switch has been either less explored or has been challenging. With the growing need for smaller computing devices with application specific capabilities, focussing on how platforms can provide better application specific computing operations using their physics can yield more efficient and powerful computing systems than using just the digital symbolic metaphor.

The need for better architectures or computational paradigms than the current status quo is driven by hard computational problems that we encounter. Such problems include associative computing, scientific computing (including solution of coupled Partial Differential Equations (PDEs)) and optimization problems. In case of hard optimization problems alternative paradigms and architectures include, but are not limited to, cellular automata [1], quantum computing [2], Ising model based systems [3], [4], neural networks [5], stochastic searching architectures [6] and memcomputing [7]. Among architectures for solving PDEs cellular neural networks (CNN) have been studied [8], [9]. Some studies have also suggested using cellular automata for solving PDEs [10].

With such growing interest in more powerful computing substrates, researchers have started looking beyond CMOS devices. Interesting devices have come up which can be used for more complex information processing than a switch using just their first principles. One such class of devices which look promising are metal-insulator-transition (MIT) devices. MIT devices based on Vanadium-Dioxide (VO_2) thin films transition from a metallic state to an insulating state based on the electric field (or voltage) applied across them. When the voltage applied increases above a threshold, the device turns into a metallic state, and when the voltage applied reduces below a threshold, it changes back to an insulating state. The thresholds are not equal and there is hysteresis in transition. This hysteresis can be used to create self-sustained oscillations [11] in a very simple circuit with a VO_2 device in series with a resistance. In Section II we present an brief background of oscillator based computing paradigms, and in Section III we describe various ways of computing using MIT based relaxation oscillators.

II. Oscillator based computing

A computing system is characterized by two basic properties - (a) Information representation, and (b) Information transformation. Information representation means how information is represented in physical form in the physical substrate. Information transformation means how dynamics of the physical medium is used to transform information from one value to another. In case of oscillators, there are multiple ways of achieving the above two.

Analog information can be represented as frequency, or phase of the oscillators. Digital information can be stored in thresholded analog forms, and also possibly bifurcations, if the circuit elements can be controlled. Information transformations can be achieved by either controlling circuit elements as above, or by coupling. Coupling is an interesting phenomenon where two or more oscillators can be connected in such a way that they affect each other's oscillations and finally the oscillators show synchronization. As such, the information is transformed in the synchronized state to some meaningful value based on an application and information representation.

978-1-5090-6182-2/17/$31.00 ©2017 IEEE

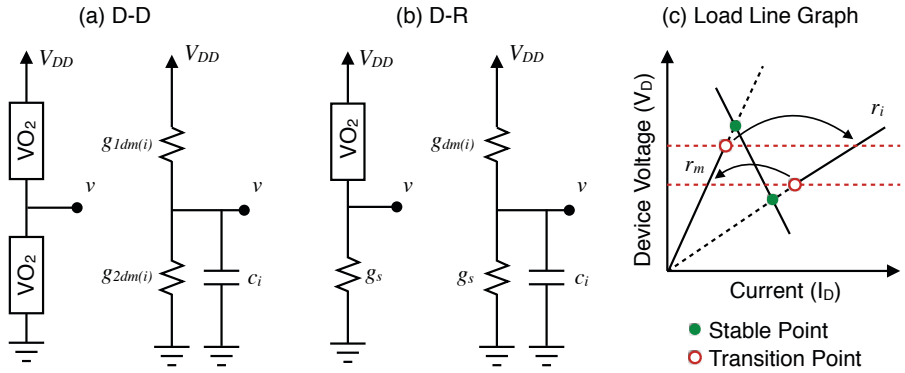

Fig. 1. (a) D-D oscillator circuit configuration and its equivalent circuit (b) D-R oscillator circuit configuration and its equivalent circuit. (c) Load line graph for the D-R circuit and the region of operation of D-R oscillator. When the stable points (green filled points) are outside the region of operation, the system shows oscillations.

A. Sinusoidal oscillators

One such oscillator model is using sinusoidal oscillators called the *Kuramoto* model [12]. In this model the oscillators are simple harmonic and their coupling is assumed to affect each other's phases linearly. If the oscillators with phases θ_1 and θ_2 have frequencies ω_1 and ω_2 then in Kuramoto models the coupling of two oscillators will result in the phase equations:

$$\dot{\theta_1} = \omega_1 + k(\theta_1 - \theta_2)$$
$$\dot{\theta_2} = \omega_2 + k(\theta_2 - \theta_1)$$

where k is the coupling constant. A *Kuramoto* system of N oscillators is described by

$$\dot{\theta_i} = \dot{\omega_i} + \frac{K}{N}\sum_{j=1}^{N}\sin(\theta_j - \theta_i), \quad i = 1, ..., N$$

where θ_i and ω_i are the phase and frequency respectively of i^{th} oscillator.

One application of such coupling which uses frequency representation in oscillators is that of frequency locking. When ω_1 and ω_2 are close, the oscillators will synchronize and finally oscillate with the same frequency which lies in between the original frequencies. But if they are not close enough, they will not synchronize. This bifurcation behavior can be used as a digital output based on the frequencies as the input. But such properties can possibly have much more interesting applications when exploited in networks of such coupled oscillators instead of just a pair of coupled oscillators.

In case of coupled networks of such oscillators, another application which uses phase representation of information is that of synchronization when oscillators have same frequency. In this case, the phases of oscillators settle down to meaningful transformations in the steady state giving rise to the so called phase based *oscillatory associative memories*. The steady state phase differences are a function of the weight matrix by which the network is connected. The weight matrix can be considered as stored memories and the steady state phase differences settle down to a limit cycle corresponding to one of the stored memories which is the closest to the initial vctor of phase differences.

Even though, in theory, these oscillators are simple and powerful, their implementation in hardware have been very difficult mainly due to the specific kind of coupling assumed in the *Kuramoto* models. This is because such coupling equations arise only in the limits of weak coupling, i.e. when the coupling strengths are very weak, and do not hold when the coupling is strong. This creates a big challenge in implementing such coupling in hardware. For instance, one effort using compact oscillators in non-silicon technologies is the use of Spin Torque Oscillators (STOs) coupled using spin diffusion currents and providing a computational platform for machine learning, spiking neural networks and others [13], [14]. However, the high current densities of STOs and the limited range of spin diffusion currents continue to pose serious challenges to technologists.

B. Non-linear oscillators

Similar models of weak linear phase coupling were also explored for Van Der Pol oscillators [15] which have an additional nonlinearity. But the implementation of such oscillators is also non-trivial and the coupling behavior becomes too complicated to tackle large connected networks [16]–[19].

III. Relaxation Oscillators

A. Metal-Insulator State Transition Devices

The relaxation oscillators we consider here are based on state switching devices made using Vanadium-Dioxide thin films which are metal-insulator-transition (MIT) devices. These devices behave effectively as linear resistances. The characteristic property of such devices is that they switch between a metallic state and an insulating state based on the voltage applied across their terminals. When the voltage applied across their terminals exceeds above a threshold, say V_h, these devices change to a metallic state. And when the voltage applied across them reduces below a threshold, say

V_l, these devices switch back to an insulating state. The thresholds V_h and V_l are not equal and there is hysteresis in transitions. An internal capacitance is associated with the device which ensures gradual buildup and decaying of the voltage (or energy) across the device. The current switches very abruptly when the device switches state.

B. MIT based oscillators

The hysteretic metal-insulator transition can be harnessed to create relaxation oscillators using very simple circuits. There are two simple configurations [20] - (a) two MIT devices in series called the D-D configuration (D stands for device), and (b) a MIT device in series with a fixed resistance, called the D-R configuration (R stands for resistance). The circuit schematics for these oscillators are shown in figure 1. We will follow the following convention for voltages in the rest of the paper. Uppercase voltage denote absolute voltages, and lowercase voltages denote that the voltage value is normalized w.r.t. V_{dd}. This means $v_l = V_l/V_{dd}$ and $v_h = V_h/V_{dd}$.

In the D-D configuration, if the devices are identical and the condition $V_l + V_h = V_{dd}$ holds then the system would oscillate if the initial states of the devices are opposite, i.e. one device is metallic and the other is insulating. This is because any time one device switches, the other will make the opposite transition as well. As $g_{dm} \gg g_{di}$, the devices can be considered as switches which are open in insulating state and closed in metallic with conductance g_{dm}. We assume $g_{di} = 0$ and a finite g_{dm}. The mechanism of oscillations is essentially charging and discharging of the internal capacitances of the devices. The device in metallic state connects the circuit and charges (discharges) the lumped internal capacitance. The voltage at the output node increases (decreases) and eventually reaches the threshold voltage. Because of the constraint on v_l and v_h as stated above, both devices will switch at the same time causing their behavior to switch. The charging (discharging) becomes discharging (charging) and the cycle continues.

The single D-D oscillator can be described by the following set of piecewise linear differential equations:

$$cv' = \begin{cases} (v_{dd} - v)g_{1dm} & charging \\ -g_{2dm} & discharging \end{cases}$$

where g_{1dm} and g_{2dm} are metallic conductances of the two devices respectively. As $g_{di} \gg g_{dm}$ there is no term involving g_{di} in the equations. The equation can be re-written as:

$$cv' = -g(s)v + p(s)$$

where s denotes the conduction state of the device (0 for metallic, and 1 for insulating) and $g(s)$ and $p(s)$ depend on the device conduction state s as follows:

$$g(s) = \begin{cases} g_{1dm}, & s = 0 \\ g_{2dm}, & s = 1 \end{cases}$$

$$p(s) = \begin{cases} g_{1dm}, & s = 0 \\ 0, & s = 1 \end{cases}$$

For D-R oscillators, the oscillations occur due to a lack of stable point as seen in the load line graph of figure 1c. Solid lines with slopes r_i and r_m are the regions of operation of the device in insulating and metallic states respectively. The system does not enter the dashed line region as a transition occurs to the other conduction state at the red points. The stable points, denoted by green points, are the points where the load line intersects the I-V curve of the device. These stable points in each state lie outside the region of operation of the circuit and hence the circuit shows self sustained oscillations. This is a much more practical configuration from an electrical implementation point of view, as the conditions required for oscillations are not very strict.

Following similar analysis as in the D-D oscillator case, the dynamics of the single D-R oscillator can be described as:

$$cv' = \begin{cases} (v_{dd} - v)g_{dm} - vg_s & charging \\ -vg_s & discharging \end{cases}$$

which can be re-written as:

$$cv' = -g(s)v + p(s)$$

where,

$$g(s) = \begin{cases} g_{dm} + g_s, & s = 0 \\ g_s, & s = 1 \end{cases}$$

$$p(s) = \begin{cases} g_{dm}, & s = 0 \\ 0, & s = 1 \end{cases}$$

and s denotes the conduction state of the system as before. Detailed analysis of configurations and modeling of such oscillators can be found in [20].

It is interesting to note that an oscillator cannot be created with first order dynamics, but an oscillator can be created using piecewise linear dynamics. In our case, if the piecewise linear dynamics arise from the state switching behavior as in the case of VO_2 devices, then the hysteresis provides that minimum necessary memory in the circuit to create oscillations without any inductance.

Experiments with VO_2: An MIT device can be realized using VO_2 (Vanadium dioxide) which exhibits unique electronic properties like metal-insulator phase transitions. VO_2 has been shown to undergo abrupt first order metal-to-insulator and insulator- to-metal transitions with up to five orders of change in conductivity [21] and ultra-fast switching times [22]. This transition can be triggered using thermal [23], optical [24], electronic [25] or strain [26] stimuli. The electrically driven first order metal-insulator-transition in VO_2 is always accompanied by hysteresis in switching as shown in figure 2a. In our experiments, the VO_2 is epitaxially grown on (001) TiO_2 (-0.86% compressive strain) using Molecular Beam Epitaxy (MBE), then patterned to form channels and followed by deposition of Au/Pd contacts to electrically access the VO_2 channel. The insulator to metal transition (IMT) and the reverse metal to insulator transition (MIT) occur at two critical fields, E_2 and E_1, respectively. Similar to what was discussed

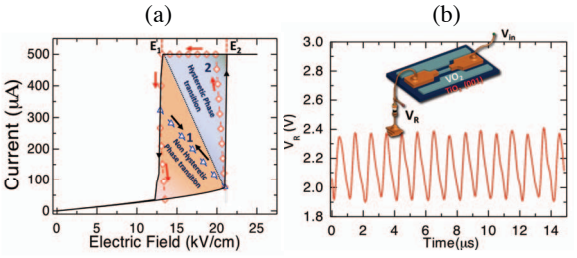

Fig. 2. (a) Measured I-E characteristics of a VO_2 device illustrating the hysteretic window (b) Measured characteristics show oscillations when biased with a pull down resistor

in the previous section, when a VO_2 device was operated in the hysteretic region with a series resistance, it breaks into spontaneous oscillations (figure 2b).

C. Information representation

Information in MIT oscillators, like sinusoidal oscillators, can be represented as phase, or frequency. Frequency of these relaxation oscillators can be interpreted as the frequency of the state transitions. Converting any analog input to a frequency representation can be done by creating a functional relationship between the input and the effective series resistance through which the internal capacitor charges. For instance, in a D-R oscillator, such a conversion can be achieved using a transistor in place of the series resistor (figure 3a). Any input applied at the gate of the transistor is converted to a frequency, although the relationship is not linear. Figure 3c shows such a non-linear relationship assuming the small signal model of the MOSFET (figure 3b). In case of phase, the information can be stored by adjusting the time of start of oscillations based on the input. The read-out of the frequency or phase can easily be done using any phase-frequency detectors (PFD). Another way of reading out relative phases of two oscillators is to threshold the outputs of oscillators and find the time average of a XOR function [27], [28].

D. Information transformation with D-D oscillators

The behavior of such oscillators when coupled provides interesting possibilities for transforming information. We focus on phase based representation in these coupled oscillators, where these oscillators are identical. The oscillators are coupled using simple passive resistive and/or capacitive circuits through their output nodes (figure 5a). It was found in [27] that the pairwise coupling behavior of D-D oscillators differ from that of D-R oscillators, therefore these coupled oscillators would find use in different applications.

Two identical D-D oscillators coupled using a RC circuit can be modeled as follows. When coupled, the system has 4 conduction states $s = s_1 s_2 \in \{00, 01, 10, 11\}$ corresponding to the 4 combinations of s_1 and s_2. The coupled system can be described in matrix form as:

$$\begin{aligned} c_c F x'(t) &= -g_c A(s) x(t) + P(s) \\ x'(t) &= -\frac{g_c}{c_c} F^{-1} A(s) \left(x(t) - A^{-1}(s) P(s) \right) \end{aligned}$$

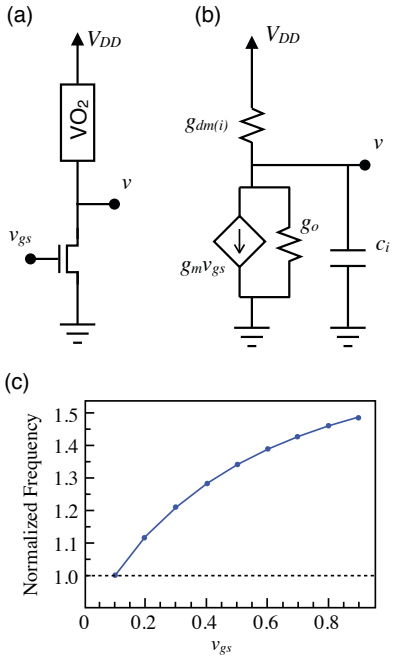

Fig. 3. (a) Oscillator circuit with MOSFET in series with a VO_2 device (b) Small signal equivalent circuit of the oscillator with VO_2 in series with a MOSFET (c) Frequency vs v_{gs} curve of the VO_2 oscillator

where $x(t) = (v_1(t), v_2(t))$ is the state variable at any time instant t. The 2×2 matrices F and $A(s)$, and vector $P(s)$ are given by:

$$F = \begin{bmatrix} 1+\alpha_1 & -1 \\ -1 & 1+\alpha_2 \end{bmatrix}$$

$$A(00) = \begin{bmatrix} -\beta_{11}-1 & 1 \\ 1 & -\beta_{21}-1 \end{bmatrix}, \quad P(00) = \begin{bmatrix} \beta_{11} \\ \beta_{21} \end{bmatrix}$$

$$A(10) = \begin{bmatrix} -\beta_{12}-1 & 1 \\ 1 & -\beta_{21}-1 \end{bmatrix}, \quad P(10) = \begin{bmatrix} 0 \\ \beta_{21} \end{bmatrix}$$

$$A(01) = \begin{bmatrix} -\beta_{11}-1 & 1 \\ 1 & -\beta_{22}-1 \end{bmatrix}, \quad P(01) = \begin{bmatrix} \beta_{11} \\ 0 \end{bmatrix}$$

$$A(11) = \begin{bmatrix} -\beta_{12}-1 & 1 \\ 1 & -\beta_{22}-1 \end{bmatrix}, \quad P(11) = 0$$

Here, $\alpha_i = c_i/c_c$ is the ratio of the combined lumped capacitance of i^{th} oscillator to the coupling capacitance c_c, and $\beta_{ij} = g_{ijdm}/g_c$ is the ratio of the metallic state resistance of j^{th} device of i^{th} oscillator, where $i \in \{1, 2\}$ and $j \in \{1, 2\}$. The fixed point in a conduction state s is given by $p_s = A^{-1}(s)P(s)$ and the matrix determining the flow (the *flow matrix* or the *velocity matrix*) is given by $\frac{g_c}{c_c} F^{-1} A(s)$.

It was shown in [27] by symmetry reduction techniques that under simple assumptions when two identical D-D oscillators with equal charging and discharging rates are coupled using a capacitance, they tend to synchronize in anti-phase locking, and when coupled using a resistance they synchronize in in-phase locking. If the coupling circuit is a parallel combination of a resistance and capacitance, the steady state locking is still either anti-phase or in-phase, but depends on the relative values

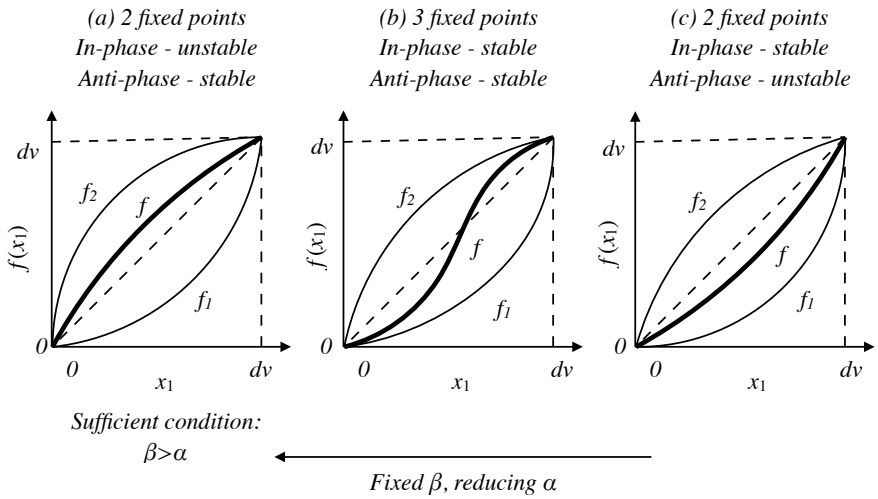

Fig. 4. Representative plot of mappings f_1, f_2 and their composition $f = f_1 \circ f_2$ with fixed β and varying α. Here, $dv = v_h v_l$. $\beta > \alpha$ is a sufficient condition for a concave f and hence stable anti-phase locking. As α increases, the curve for f transitions into a s-shaped curve with both in-phase and anti-phase lockings stable, and then finally to a convex curve with stable in-phase locking.

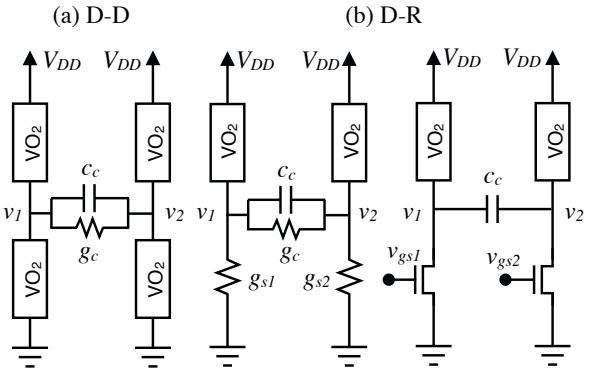

Fig. 5. D-D (a) and D-R (b) coupled oscillator circuits using parallel RC circuit as the coupling circuit.

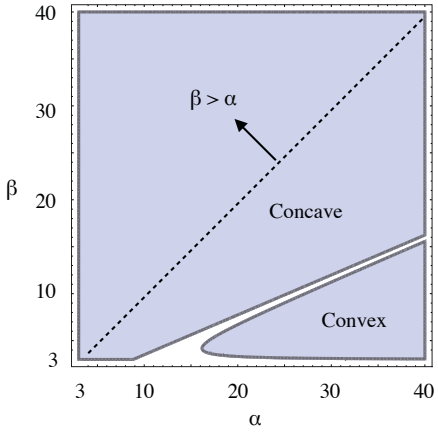

Fig. 6. Return map type for the symmetric D-D case in the parametric space $\beta \times \alpha$ for $v_l = 0.2$ and $v_h = 0.8$. We can clearly see that for $\beta > \alpha$ the return map is concave and anti-phase locking is stable. When the coupling is more resistive, the return map becomes convex with stable in-phase locking. The region between concave and convex return map is the region with S-shaped return map with both stable in-phase and stable anti-phase locking.

of the coupling resistance and capacitance. The symmetry reduced return map of the coupled system can be decomposed as the composition of two 1-dimensional functions - a concave function f_2 and a convex function f_1. In case the coupling has more capacitive element, the resulting function from composition is a concave function with stable anti-phase locking and unstable in-phase locking (figure 4a). In case the coupling is more resistive, the return map is convex with stable in-phase locking and unstable anti-phase locking (figure 4c). Interestingly, if the coupling resistance and capacitance are tuned to go from resistive coupling to capacitive coupling, instead of an abrupt switching from convex to a concave return map, there is a region where the return map is S-shaped where both in-phase and anti-phase locking is stable (figure 4b). In this bistable region there is another unstable periodic orbit which is neither anti-phase nor in-phase. It was proved in [20] that a sufficient condition for a concave return map is $\beta > \alpha$.

The kinds of return map in coupled D-D oscillators are visualized in the parameter space $\alpha - \beta$ in figure 6. The two regions for concave and convex return map can be clearly seen. They are separated by a thin region which represents the case of bistability.

Such characteristics can be very useful in phase-based representation and transformation. A coupled D-D oscillator system can be configured by controlling the parameters α and β to always yield in-phase output, out-of-phase output, or either of these depending on the initial relative phase of the oscillators. For non-identical oscillators, or even non-identical devices in a single oscillator, the analysis becomes difficult. Although D-D oscillator coupling provides interesting behaviors which can be utilized for a variety of possible computing paradigms and

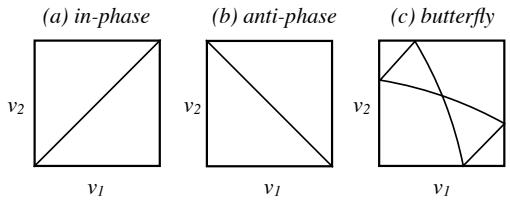

Fig. 7. Steady state trajectories of coupled oscillators with outputs v_1 and v_2 settle to the diagonals in case of identical D-D coupling for in-phase locking (a) and anti-phase locking (b). In case of identical D-R oscillators, the trajectories settle to a butterfly shaped curve as seen in (c).

provides a good substrate for theoretical interest, the practical implementation of such oscillators is difficult in the current state.

E. Information transformation with D-R oscillators

Similar to D-D oscillators, a symmetry reduction technique was used for analyzing D-R oscillators [27]. Contrary to D-D oscillators, D-R oscillators do not have equal charging and discharging rates. As such, the analyses becomes difficult as there is one less symmetry. It can be shown that under simple assumptions in case of coupled identical D-R oscillators, the return map of the system can be written as the piecewise composition of four 1-dimensional functions. As a general observation, when the charging processes are very fast compared to the discharging processes (which is true in the fabricated VO_2 oscillators), the oscillators tend to lock anti-phase when coupled using a capacitor. This anti-phase locking in D-R oscillators differs fundamentally from the anti-phase locking in the symmetric D-D case. Considering only identical oscillators as in the previous case of coupled D-D oscillators, if the phase portraits, i.e. trajectory of the system in the $v_1 \times v_2$ place is observed, we see that in the symmetric D-D case the anti-phase locking is a ideal (figure 7b) whereas in the D-R case the anti-phase locking comes from a butterfly shaped phase-portrait (figure 7c). In time domain, the butterfly-shaped curve represents non-monotonic discharging state of the oscillators with kinks. If the charging processes are very fast compared to discharging processes, the kinks are small, and the butterfly shaped phase portraits stay close to the anti-phase diagonal.

When the oscillators are non-identical, i.e. their fundamental frequencies are different, they show properties similar to other oscillators like that of locking within a locking range and can be used for computing applications as well. Their compact low power implementation make them an attractive for creating large coupled arrays of oscillators and for computing applications. Given the practicality of implementing D-R oscillators in hardware, they provide us with a powerful and scalable platform to compute. Interesting applications have been explored for both frequency based representations and phase based representations.

Experiments with VO_2: Experiments using VO_2 for coupled D-R oscillators were demonstrated for both types - with a series resistance [11], and with a series MOSFET [28]. Circuit schematics for these circuits are shown in Figure 5b. Figure 8

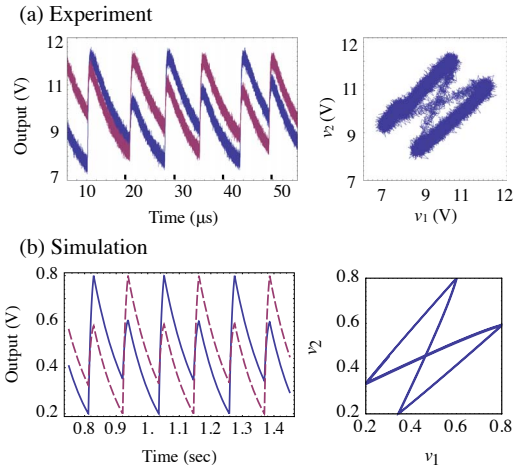

Fig. 8. Experimental and simulated time domain waveforms in the steady state and phase plots for a parallel RC coupled D-R oscillator system. The two waveforms show close match and validate the model prediction.

shows the butterfly shaped steady state orbits in the D-R coupled oscillator system and a close match can be seen between the expermintal and the simulated waveforms validating the models developed for MIT based D-R oscillators.

F. Applications of D-R oscillators

1) Frequency based representation: The property of locking and locking range can be used when using frequency based representation of information. If the frequency of oscillators is controlled using the gate voltage of a series transistor (figure 3a), then a pair of such coupled oscillators (figure 5b) can be used as a comparator for comparing the two gate voltages of the series transistors of the coupled oscillators based on its locking state. Interestingly, we can extract more information than just the locking state of the oscillators. The steady state relative phase of the oscillators (or the steady state periodic orbits) change in a predictable manner as a function of the difference of gate voltages of the coupled oscillators as was shown in [27], [28]. Let us consider the *XOR method* of measuring the steady state phase difference of oscillators. In this method, first the oscillator outputs are thresholded at 0.5 and converted to a binary signal. Next, a XOR operation is performed at each time instant on this thresholded value of oscillators. Finally, a time average is taken for the resulting output. In terms of the phase domain $v_1 \times v_2$, the *XOR method* is equivalent to the fraction of time the trajectory spends in the gray regions as shown in figure 9. For $v_{gs1} = v_{gs2}$ the steady state trajectory is a symmetric butterfly with almost not part in the gray regions. As $v_{gs1} - v_{gs2}$ increases in magnitude, the steady state orbit is distorted and the system spends more time in the gray regions contributing to an increased value of the averaged XOR operation. Experiments [28] show similar XOR curves to what the theory and simulations indicate (figure 10a,b). The value of averaged XOR as a function of v_{gs1} and v_{gs2} is shown in figure 10c. As can be seen, the averaged XOR value is minimum along the line $v_{gs1} = v_{gs2}$ and increases as

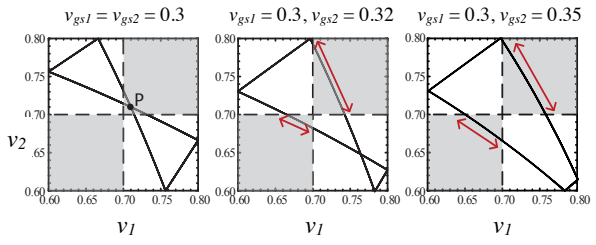

Fig. 9. Relationship between XOR output and the steady state periodic orbit of the system. At any time instant, XOR output is 1 in the gray region and 0 otherwise. Averaged XOR output is equal to the fraction of time spent by the system in the gray regions. XOR output is minimum in case of a butterfly shaped orbit (left) and should increase as the orbit transitions to a rectangular orbit (right)

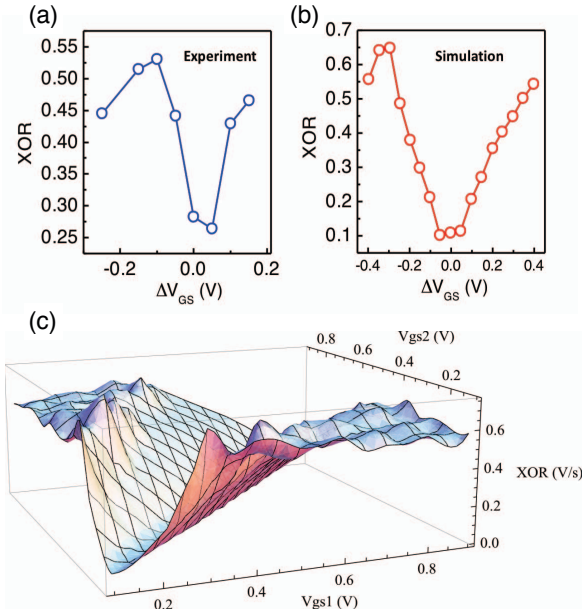

Fig. 10. (a,b) Experimental results and simulations reveal the capability of coupled oscillator phases to encode a measure of difference between two inputs ΔV_{GS} (c) Averaged XOR output as a function of v_{gs1} and v_{gs2}

the difference increases till a certain limit which is the locking range, beyond which the the oscillators cease to lock and the averaged XOR measure settles to some value close to 0.5.

A coupled VO_2-MOSFET configuration cascaded with a XOR provides a way of measuring a form of fractional distance using FSK. Arrays of such oscillators can be used for template matching where pairwise differences can also give sufficient information for matching. An example template matching application is shown in figure 11a. It was found using simulations that coupled oscillators provide a power reduction of 20X over 11 nm CMOS node reflecting the advantage of let physics do the computing approach. Another application for such coupled oscillator comparator is saliency detection at the sensor frontend where the difference of nearby pixels in a image can be computed using such oscillator arrays (figure 11b). For further details interested readers are pointed to the

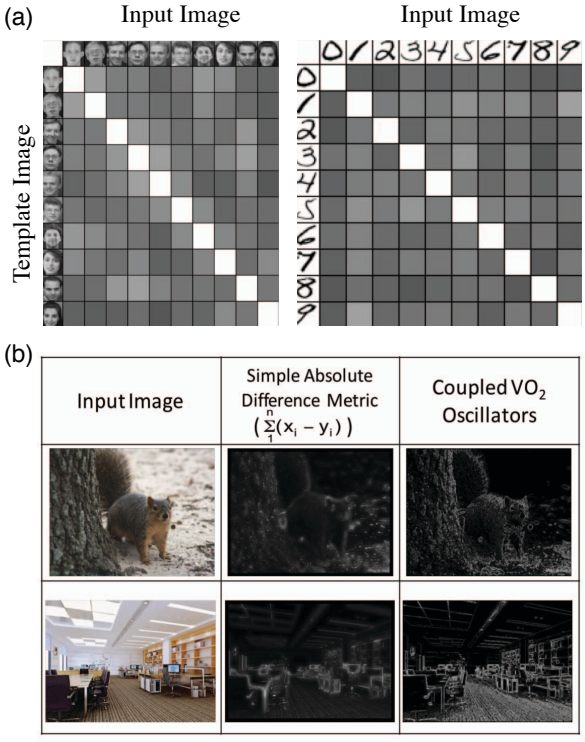

Fig. 11. (a) Pairwise XOR measure is extended to illustrate pattern matching between an input and a template. A lighter color corresponds to a better match. (b) Saliency detection of images using coupled oscillator systems and a digital implementation

previous work by the authors [28].

2) Phase based representation: An interesting phase based applications for D-R oscillators has been demonstrated theoretically and experimentally in [29] for approximating the solution of NP-hard graph coloring problem. Unlike previous applications which had only pairwise coupling, here the oscillators are connected in a global network that corresponds to the graph whose coloring is desired. When n identical D-R oscillators are coupled using identical capacitors, such network settles to a steady state wherein the relative phases of the oscillators get ordered in a way that corresponds to the solution of graph coloring. The time evolution of the piecewise linear dynamical system of such coupled D-R oscillators inherits the properties of and hence mimics approximate graph coloring algorithms because of the construction of such networks. Basic functioning of such a system is shown in Fig. 12.

IV. Conclusion

In this article we review various computational paradigms based on the dynamics that evolve from interactions between relaxation oscillators made using hysteretic metal-insulator-transition (MIT) devices. Hardware implementation and fabrications of such oscillators using VO_2, as well as coupled networks of such oscillators, have been demonstrated experimentally in various works referred to in the paper. Such oscillators are compact and their coupling behavior has been

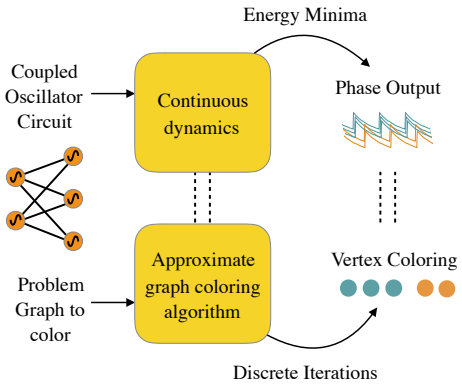

Fig. 12. Overview of proposed graph coloring system using coupled VO_2 oscillators where each node correspond to a VO_2 oscillator. The dynamics of system follows an approximate graph coloring algorithm and the steady state phase outputs of VO_2 oscillators can be used to color nodes of the graph.

well modeled in theory as shown in this article along with various works mentioned. It is a big step towards using post-CMOS devices to build computing systems that are not based on just "switches" and which use complex interactions and dynamics of coupled oscillators to do meaningful computation. This also has a lot of advantages in terms of energy efficiency and performance of computing in the post-CMOS world.

Acknowledgements

This project was supported by the National Science Foundation under grant 1640081, and the Nanoelectronics Research Corporation (NERC), a wholly-owned subsidiary of the Semiconductor Research Corporation (SRC), through Extremely Energy Efficient Collective Electronics (EXCEL), an SRC-NRI Nanoelectronics Research Initiative under Research Task ID 2698.002.

References

[1] S. Wolfram, *Theory and applications of cellular automata: including selected papers, 1983-1986*. No. v. 1 in Advanced series on complex systems, Singapore: World Scientific, 1986.

[2] P. Shor, "Polynomial-Time Algorithms for Prime Factorization and Discrete Logarithms on a Quantum Computer," *SIAM Journal on Computing*, vol. 26, pp. 1484–1509, Oct. 1997.

[3] A. Lucas, "Ising formulations of many NP problems," *Interdisciplinary Physics*, vol. 2, p. 5, 2014.

[4] Z. Wang, A. Marandi, K. Wen, R. L. Byer, and Y. Yamamoto, "Coherent Ising machine based on degenerate optical parametric oscillators," *Physical Review A*, vol. 88, p. 063853, Dec. 2013.

[5] J. J. Hopfield and D. W. Tank, ""Neural" computation of decisions in optimization problems," *Biological Cybernetics*, vol. 52, pp. 141–152, July 1985.

[6] H. Mostafa, L. K. Müller, and G. Indiveri, "An event-based architecture for solving constraint satisfaction problems," *Nature Communications*, vol. 6, p. 8941, Dec. 2015.

[7] F. L. Traversa, C. Ramella, F. Bonani, and M. Di Ventra, "Memcomputing NP-complete problems in polynomial time using polynomial resources and collective states," *Science Advances*, vol. 1, pp. e1500031–e1500031, July 2015.

[8] L. O. Chua and L. Yang, "Cellular neural networks: applications," *IEEE Transactions on Circuits and Systems*, vol. 35, pp. 1273–1290, Oct. 1988.

[9] L. O. Chua and L. Yang, "Cellular neural networks: theory," *IEEE Transactions on Circuits and Systems*, vol. 35, pp. 1257–1272, Oct. 1988.

[10] T. Toffoli, "Cellular automata as an alternative to (rather than an approximation of) differential equations in modeling physics," *Physica D: Nonlinear Phenomena*, vol. 10, pp. 117–127, Jan. 1984.

[11] N. Shukla, A. Parihar, E. Freeman, H. Paik, G. Stone, V. Narayanan, H. Wen, Z. Cai, V. Gopalan, R. Engel-Herbert, D. G. Schlom, A. Raychowdhury, and S. Datta, "Synchronized charge oscillations in correlated electron systems," *Scientific Reports*, vol. 4, May 2014.

[12] S. H. Strogatz, "From Kuramoto to Crawford: exploring the onset of synchronization in populations of coupled oscillators," *Physica D: Nonlinear Phenomena*, vol. 143, no. 1, pp. 1–20, 2000. read.

[13] K. Yogendra, D. Fan, and K. Roy, "Coupled spin torque nano oscillators for low power neural computation," *IEEE Transactions on Magnetics*, vol. 51, pp. 1–9, Oct 2015.

[14] A. Sengupta, P. Panda, P. Wijesinghe, Y. Kim, and K. Roy, "Magnetic tunnel junction mimics stochastic cortical spiking neurons," *Scientific Reports*, vol. 6, pp. 30039 EP –, 07 2016.

[15] B. Van Der Pol, "The Nonlinear Theory of Electric Oscillations," *Proceedings of the Institute of Radio Engineers*, vol. 22, no. 9, pp. 1051–1086, 1934.

[16] R. H. Rand and P. J. Holmes, "Bifurcation of periodic motions in two weakly coupled van der Pol oscillators," *International Journal of Non-Linear Mechanics*, vol. 15, no. 4–5, pp. 387–399, 1980.

[17] D. W. Storti and R. H. Rand, "Dynamics of two strongly coupled van der pol oscillators," *International Journal of Non-Linear Mechanics*, vol. 17, no. 3, pp. 143–152, 1982.

[18] N. Kopell and D. Somers, "Anti-phase solutions in relaxation oscillators coupled through excitatory interactions," *Journal of Mathematical Biology*, vol. 33, pp. 261–280, Dec. 1995.

[19] N. Hirano and S. Rybicki, "Existence of limit cycles for coupled van der Pol equations," *Journal of Differential Equations*, vol. 195, pp. 194–209, Nov. 2003.

[20] A. Parihar, N. Shukla, S. Datta, and A. Raychowdhury, "Synchronization of pairwise-coupled, identical, relaxation oscillators based on metal-insulator phase transition devices: A model study," *Journal of Applied Physics*, vol. 117, p. 054902, Feb. 2015.

[21] L. A. Ladd and W. Paul, "Optical and transport properties of high quality crystals of v 2 o 4 near the metallic transition temperature," *Solid State Communications*, vol. 7, no. 4, pp. 425–428, 1969.

[22] A. Kar, N. Shukla, E. Freeman, H. Paik, H. Liu, R. Engel-Herbert, S. Bharadwaja, D. G. Schlom, and S. Datta, "Intrinsic electronic switching time in ultrathin epitaxial vanadium dioxide thin film," *Applied Physics Letters*, vol. 102, no. 7, p. 072106, 2013.

[23] M. M. Qazilbash, M. Brehm, B.-G. Chae, P.-C. Ho, G. O. Andreev, B.-J. Kim, S. J. Yun, A. V. Balatsky, M. B. Maple, F. Keilmann, H.-T. Kim, and D. N. Basov, "Mott transition in vo2 revealed by infrared spectroscopy and nano-imaging," *Science*, vol. 318, no. 5857, pp. 1750–1753, 2007.

[24] A. Cavalleri, C. Tóth, C. W. Siders, J. A. Squier, F. Ráksi, P. Forget, and J. C. Kieffer, "Femtosecond structural dynamics in vo_2 during an ultrafast solid-solid phase transition," *Phys. Rev. Lett.*, vol. 87, p. 237401, Nov 2001.

[25] B.-J. Kim, Y. W. Lee, S. Choi, J.-W. Lim, S. J. Yun, H.-T. Kim, T.-J. Shin, and H.-S. Yun, "Micrometer x-ray diffraction study of vo_2 films: Separation between metal-insulator transition and structural phase transition," *Phys. Rev. B*, vol. 77, p. 235401, Jun 2008.

[26] CaoJ., ErtekinE., SrinivasanV., FanW., HuangS., ZhengH., Y. W. L., K. R., O. F., G. C., and WuJ., "Strain engineering and one-dimensional organization of metal-insulator domains in single-crystal vanadium dioxide beams," *Nat Nano*, vol. 4, pp. 732–737, 11 2009.

[27] A. Parihar, N. Shukla, S. Datta, and A. Raychowdhury, "Exploiting Synchronization Properties of Correlated Electron Devices in a Non-Boolean Computing Fabric for Template Matching," *IEEE Journal on Emerging and Selected Topics in Circuits and Systems*, vol. PP, no. 99, pp. 1–10, 2014.

[28] N. Shukla, A. Parihar, M. Cotter, M. Barth, X. Li, N. Chandramoorthy, H. Paik, D. Schlom, V. Narayanan, A. Raychowdhury, and S. Datta, "Pairwise coupled hybrid vanadium dioxide-MOSFET (HVFET) oscillators for non-boolean associative computing," in *Electron Devices Meeting (IEDM), 2014 IEEE International*, pp. 28.7.1–28.7.4, Dec. 2014.

[29] A. Parihar, N. Shukla, M. Jerry, S. Datta, and A. Raychowdhury, "Vertex coloring of graphs via phase dynamics of coupled oscillatory networks," *ArXiv e-prints*, Sept. 2016.